Science Translational Medicine
AAAS

Methylation Subtypes and Large-Scale Epigenetic Alterations in Gastric Cancer

Hermioni Zouridis *et al.*

Sci Transl Med **4**, 156ra140 (2012);
DOI: 10.1126/scitranslmed.3004504

Editor's Summary

The Silent Treatment of Gastric Cancer

A new study by Zouridis and colleagues refutes the old adage that "silence is golden"—at least in the realm of gene methylation and epigenetic silencing in cancer. To decipher the effects of "silence" on gastric cancer, the authors analyzed gene methylation patterns in 240 gastric tumors and compared them to those of 94 matched samples of adjacent normal tissue.

Gastric cancer is one of the most common types of cancer worldwide—and one of the most deadly, with few effective treatment options available. As a possible source of therapeutic targets, scientists are searching for genetic and epigenetic alteration patterns characteristic of these tumors. Here, the authors extensively characterized methylation patterns in human gastric cancers, which revealed tumor-specific arrangements of hyper- and hypomethylation. Zouridis and colleagues also identified a subset of cancers that fell into the CpG island methylator phenotype (CIMP) subgroup, which is associated with more extensive methylation and lower chances of survival in younger patients. As a possible pharmaceutical intervention, the authors tested the effects of the demethylating drug 5-aza-2′-deoxycytidine in CIMP tumor cell lines and found that their proliferation was significantly decreased when compared with non-CIMP cell lines.

A broader analysis of gene regions that undergo modifications in cancers likely will identify new therapeutic targets and corresponding treatments. But for patients with high-risk gastric cancers that fall into the CIMP subgroup, silenced DNA is golden because it serves as a target for currently available drugs.

Science Translational Medicine (print ISSN 1946-6234; online ISSN 1946-6242) is published weekly, except the last week in December, by the American Association for the Advancement of Science, 1200 New York Avenue NW, Washington, DC 20005.

GASTRIC CANCER

Methylation Subtypes and Large-Scale Epigenetic Alterations in Gastric Cancer

Hermioni Zouridis,[1]*† Niantao Deng,[1,2]* Tatiana Ivanova,[1] Yansong Zhu,[1] Bernice Wong,[3] Dan Huang,[4] Yong Hui Wu,[1,5] Yingting Wu,[6,7] Iain Beehuat Tan,[2,8] Natalia Liem,[9] Veena Gopalakrishnan,[1] Qin Luo,[1] Jeanie Wu,[5] Minghui Lee,[5] Wei Peng Yong,[9,10] Liang Kee Goh,[1] Bin Tean Teh,[1,3,4] Steve Rozen,[6,11] Patrick Tan[1,5,9,12]‡

Epigenetic alterations are fundamental hallmarks of cancer genomes. We surveyed the landscape of DNA methylation alterations in gastric cancer by analyzing genome-wide CG dinucleotide (CpG) methylation profiles of 240 gastric cancers (203 tumors and 37 cell lines) and 94 matched normal gastric tissues. Cancer-specific epigenetic alterations were observed in 44% of CpGs, comprising both tumor hyper- and hypomethylation. Twenty-five percent of the methylation alterations were significantly associated with changes in tumor gene expression. Whereas most methylation-expression correlations were negative, several positively correlated methylation-expression interactions were also observed, associated with CpG sites exhibiting atypical transcription start site distances and gene body localization. Methylation clustering of the tumors revealed a CpG island methylator phenotype (CIMP) subgroup associated with widespread hypermethylation, young patient age, and adverse patient outcome in a disease stage–independent manner. CIMP cell lines displayed sensitivity to 5-aza-2′-deoxycytidine, a clinically approved demethylating drug. We also identified long-range regions of epigenetic silencing (LRESs) in CIMP tumors. Combined analysis of the methylation, gene expression, and drug treatment data suggests that certain LRESs may silence specific genes within the region, rather than all genes. Finally, we discovered regions of long-range tumor hypomethylation, associated with increased chromosomal instability. Our results provide insights into the epigenetic impact of environmental and biological agents on gastric epithelial cells, which may contribute to cancer.

INTRODUCTION

Gastric cancer (gastric adenocarcinoma) is the second leading cause of global cancer mortality (*1*) and is particularly prevalent in Asian countries (*2*). Most gastric cancer patients present with advanced-stage disease (*3*), with the possible exception of patients in Japan and Korea where screening programs with barium photofluorography or endoscopy allow earlier detection (*3*). For patients with operable disease, conventional surgery and chemotherapy regimens are indicated, but overall 5-year survival rates of gastric cancer patients still remain at ~20% (*4*). Identifying molecular aberrations in gastric cancer may improve our understanding of gastric carcinogenesis, identify strategies for subdividing patients into biologically and clinically relevant subgroups, and highlight novel therapeutic opportunities.

Gastric tumors can display somatic mutations (*5*), genomic amplifications (7q, 8p, and 17q), and deletions (5q, 6p, and 18q) (*6*). Besides changes in DNA sequence, epigenetic alterations (DNA methylation and histone acetylation/methylation) can also influence tumor development. CG dinucleotide (CpG) methylation is frequently associated with tumor suppressor gene silencing (*7*, *8*), and CpG island (CGI) hypermethylation in gene promoters has been associated with transcriptional silencing in cancer (*7*). In gastric cancer, previous methylation studies have identified genes epigenetically silenced in gastric tumors, such as *MLH1* and *CDKN2A* (*9*–*11*). However, most previous gastric cancer methylation studies have analyzed individual genes, limited numbers of methylation markers, and relatively small patient cohorts (*9*–*11*). There thus remains a need to comprehensively define the repertoire of DNA methylation events associated with gastric cancer on a genome-wide scale and across a large, clinically annotated patient series.

Recent technologies enabling global DNA methylome analysis have been used in various cancer types to elucidate epigenetic subtypes (*12*, *13*), DNA methylation alterations associated with CGI "shores" (*14*), and long-range regions of epigenetic silencing (LRESs) (*15*). Motivated by these previous studies, we initiated an effort to characterize the gastric cancer methylome on a genome-wide scale by profiling ~300 gastric tissues (203 tumors and 94 matched normal gastric tissues) on Illumina Infinium methylation arrays. Our goal in this study was threefold. First, we sought to comprehensively describe patterns of tumor-associated DNA methylation in primary gastric cancers. Second, we investigated whether the methylation data might identify specific molecular subgroups of gastric cancer with clinical or therapeutic implications. Finally, we explored whether the methylation data might reveal large-scale epigenetic events that might have been missed in previous gastric cancer methylation studies relying on more restricted panels of methylation markers.

[1]Cancer and Stem Cell Biology Program, Duke-NUS Graduate Medical School, 8 College Road, Singapore 169857, Singapore. [2]NUS Graduate School for Integrative Sciences and Engineering, National University of Singapore, 5 Lower Kent Ridge Road, Singapore 119074, Singapore. [3]National Cancer Centre Singapore–Van Andel Research Institute Translational Research Laboratory, Department of Medical Sciences, National Cancer Centre, 11 Hospital Drive, Singapore 169610, Singapore. [4]Laboratory of Cancer Genetics, Van Andel Research Institute, Grand Rapids, MI 49503, USA. [5]Cellular and Molecular Research, National Cancer Centre, Singapore 169610, Singapore. [6]Neuroscience and Behavioural Disorders, Duke-NUS Graduate Medical School, Singapore 169857, Singapore. [7]Singapore-MIT Alliance, National University of Singapore, Singapore 119074, Singapore. [8]Division of Medical Oncology, National Cancer Centre, Singapore 169610, Singapore. [9]Cancer Science Institute of Singapore, National University of Singapore, Singapore 119074, Singapore. [10]National Cancer Institute Singapore, National University Hospital, Singapore 119228, Singapore. [11]Department of Psychiatry and Behavioral Sciences, Duke University Medical Center, Durham, NC 27710, USA. [12]Genome Institute of Singapore, 60 Biopolis Street, Genome 02-01, Singapore 138672, Singapore.
*These authors contributed equally to this work.
†Present address: LabConnect, LLC, 2910 First Avenue South, Suite 200, Seattle, WA 98134, USA.
‡To whom correspondence should be addressed. E-mail: gmstanp@duke-nus.edu.sg

RESULTS

Widespread nature of gastric cancer–specific methylation alterations

We analyzed 203 gastric tumors, 94 matched nonmalignant gastric samples ("normals"), and 37 gastric cancer cell lines on Infinium methylation arrays, measuring DNA methylation levels of 27,578 CpG sites in the human genome. The clinical features of this patient cohort are given in table S1. The CpG sites were localized primarily to 14,495 gene promoters (*16*), with 73% of the CpG sites corresponding to CGIs. To technically validate the Infinium array, we correlated the Infinium methylation profiles of 26 cell lines against profiles of the same lines generated by GoldenGate methylation arrays, an earlier validated technology interrogating a smaller number of CpG sites (~1500). We observed good levels of concordance between sites measured by both technologies (R = ~0.91; fig. S1 and table S2).

Infinium arrays quantify DNA methylation using a "β value" from 0 to 1 (0 being unmethylated) (*17*, *18*). Consistent with widespread DNA methylation differences between primary tumors and matched normal samples, unsupervised clustering analysis of the 297 primary samples revealed that most of the tumors (89%) clustered into distinct subgroups separate from most of the normal samples (93%) (fig. S2). Collectively, 11,740 CpGs were differentially methylated between tumors and normals, corresponding to 8541 genes and 44% of all autosomal CpGs ($P < 0.05$, two-sided t test, Bonferroni-corrected) (Fig. 1A). Most of the differentially methylated CpGs (83%) were hypermethylated in tumors (Fig. 1B). However, we also observed tumor-specific hypomethylation, corresponding to 17% of the differentially methylated CpGs (Fig. 1B). The average degree of tumor-specific hypomethylation was significantly greater than the average degree of tumor-specific hypermethylation ($P < 2.2 \times 10^{-16}$, Wilcoxon rank sum test).

We elected to analyze all 11,740 CpGs identified as being differentially methylated between the 203 gastric tumors and the 94 matched normal samples. Of 2766 gene promoters with multiple differentially methylated CpGs, almost all (92%; 2555 of 2766 promoters) exhibited hyper- or hypomethylation exclusively, indicating that CpG methylation is highly correlated in promoters (*19*). CpG sites hypermethylated in gastric tumors were preferentially located in CGIs ($P < 2.2 \times 10^{-16}$, χ^2 test) (Fig. 1C), whereas hypomethylated CpG sites were in non-CGI regions ($P < 2.2 \times 10^{-16}$, χ^2 test) (Fig. 1C). CpG sites exhibiting tumor hypermethylation were also located closer to transcription start sites (TSSs) than hypomethylated CpGs ($P = 5.3 \times 10^{-9}$, Wilcoxon rank sum test) (Fig. 1D). CGIs containing hypermethylated CpGs were also located significantly closer to TSSs compared to CGIs with hypomethylated CpGs ($P = 1.74 \times 10^{-8}$, Wilcoxon rank sum test) (Fig. 1E). Similar patterns were observed when the analysis was confined to only the 94 tumors with matched normal samples.

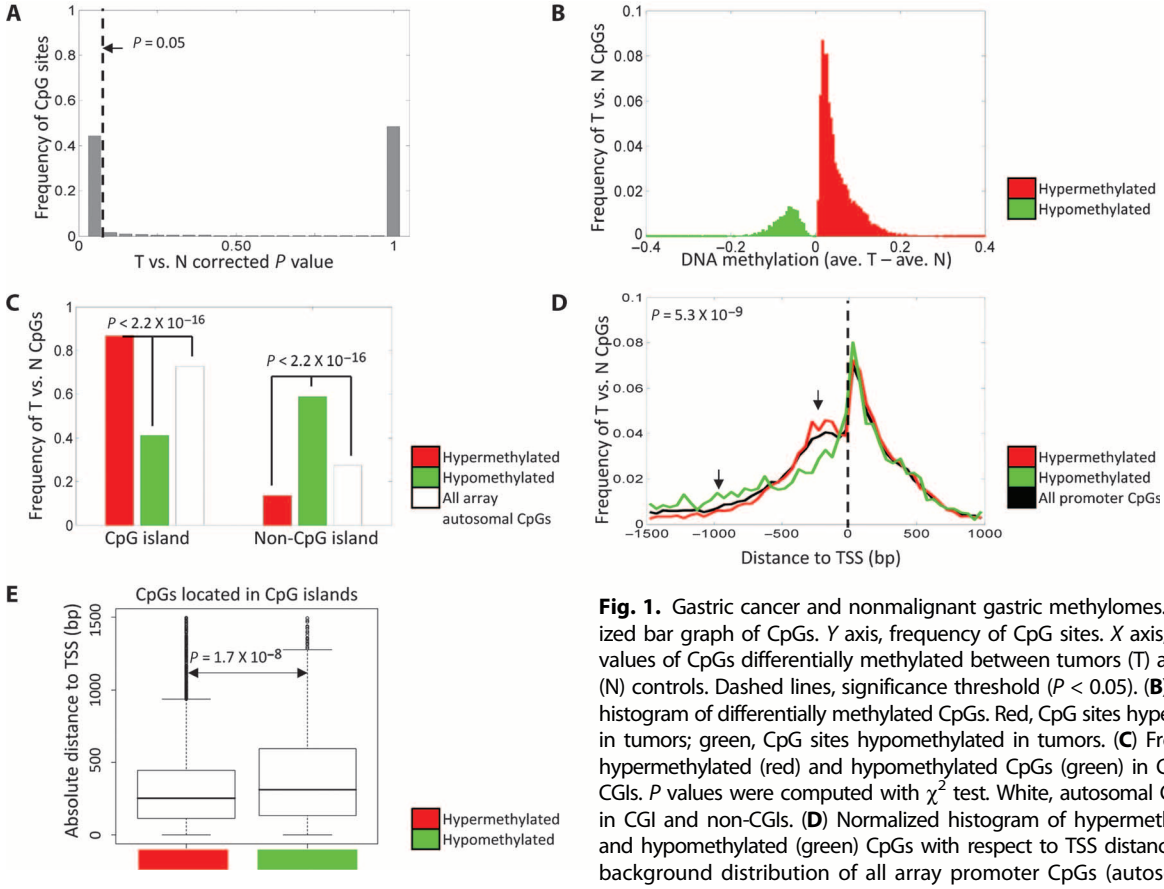

Fig. 1. Gastric cancer and nonmalignant gastric methylomes. (**A**) Normalized bar graph of CpGs. *Y* axis, frequency of CpG sites. *X* axis, corrected *P* values of CpGs differentially methylated between tumors (T) and matched (N) controls. Dashed lines, significance threshold ($P < 0.05$). (**B**) Normalized histogram of differentially methylated CpGs. Red, CpG sites hypermethylated in tumors; green, CpG sites hypomethylated in tumors. (**C**) Frequencies of hypermethylated (red) and hypomethylated CpGs (green) in CGI and non-CGIs. *P* values were computed with χ^2 test. White, autosomal CpGs located in CGI and non-CGIs. (**D**) Normalized histogram of hypermethylated (red) and hypomethylated (green) CpGs with respect to TSS distance. Black line, background distribution of all array promoter CpGs (autosomal); black arrows, deviations from the background. Upstream and downstream distances are represented by negative and positive values, respectively. *P* values were computed with the Wilcoxon rank sum test. (**E**) Box plot of TSS absolute distance for hypermethylated promoter CpGs located in CGIs (red) and hypomethylated promoter CpGs located in CGIs (green).

Influence of gastric cancer–associated methylation on gene expression

We investigated the impact of the cancer-associated methylation alterations on tumor gene expression, combining methylation and gene expression information for 223 samples (161 tumors and 62 nonmalignant samples) (*20*). Focusing our analysis on cis interactions (CpG sites and their nearest-neighbor genes), we analyzed genes exhibiting significant methylation alterations between tumors and nonmalignant controls, and for which we had gene expression data (fig. S3). Comparing 6745 CpG sites across 4903 associated genes, we identified 1653 CpGs (25%) with significant cis methylation-expression correlations ($P < 0.05$, Benjamini and Hochberg–corrected).

Seventy-eight percent of the identified methylation-expression correlations were negative, consistent with DNA methylation acting to silence local transcription (Fig. 2, A and B). These CpG sites were primarily located in promoter regions (97.7%). Genes hypermethylated and underexpressed in tumors included *MT3*, previously identified as hypermethylated and underexpressed in gastric cancer (*21*), and *PSCA*, a known gastric cancer susceptibility gene (*22*) (Table 1A). Gene set enrichment analysis (GSEA) (*23*) revealed that genes hypermethylated and underexpressed in gastric cancers were also significantly enriched in mitochondrial genes (*24*) (corrected $P < 0.05$) and genes previously reported to be down-regulated in gastric cancers from an independent study (*25*) (corrected $P = 1.66 \times 10^{-13}$) (table S3).

Conversely, genes hypomethylated and overexpressed in tumors included imprinted genes (*H19*), as well as genes involved in adhesion (*CEACAM5* and *CEACAM6*), growth promotion (*LIF*), and extracellular matrix breakdown (*MMP1*) (Table 1B). Hypomethylated/overexpressed genes were also significantly enriched in genes up-regulated in gastric cancer (*25*) (corrected $P = 5.31 \times 10^{-6}$) and those involved in cell migration (*26*) (corrected $P = 2.33 \times 10^{-5}$) (table S4).

We also observed a sizeable proportion (22%) of positively correlated methylation-expression relationships, where increased DNA methylation was associated with increased gene expression (Fig. 2B). Most of the positively correlated CpGs were also located in promoter regions (92%, 335 of 363); however, our analysis suggests that they might be associated with atypical TSS distances compared to negatively correlated CpGs. Specifically, CpGs exhibiting tumor hypermethylation and increased expression were located further upstream of TSSs compared to their cognate negatively correlated CpGs ($P = 1.4 \times 10^{-4}$, Wilcoxon rank sum test), whereas positively correlated CpG sites with tumor hypomethylation and low expression tended to lie closer to TSSs ($P = 0.08$, Wilcoxon rank sum test) (Fig. 2C). GSEA revealed that positively correlated hypermethylated CpGs located >450 base pairs (bp) upstream from TSSs overlapped with genes exhibiting *HDAC3*-dependent transcription (*27*) (corrected $P = 0.04$), whereas positively correlated hypomethylated CpGs significantly overlapped with genes related to *EZH2* (*28*), a Polycomb group protein involved in transcriptional silencing [corrected $P = 0.03$; 11 of 52 genes (~20%)]. It is possible that for these positively correlated CpGs, transcriptional regulation may be dominated by epigenetic mechanisms other than DNA methylation. Integration of the positively correlated CpGs with in-house chromatin mark data of primary gastric tumors also suggests that some of these CpGs may occupy cryptic promoters (fig. S4 and table S5).

Our analysis also revealed that, besides promoters, positively correlated CpGs were significantly more likely to be located within gene bodies ($P < 2.2 \times 10^{-16}$, χ^2 test) (Fig. 2D and table S6). Genes exhibiting gene body hypermethylation and overexpression in tumors included *RB1*, and genes exhibiting gene body hypomethylation and underexpression in tumors included *SEMA3B* (Fig. 2E). Intriguingly, several genes exhibiting positively correlated gene body CpGs have previously been implicated in cancer, including *CDKN2A*, *RUNX3*, *RB1*, *BCL2*, and *ATM*. Genes exhibiting positive methylation–gene expression correlations in gene bodies also were significantly more likely to exhibit negative correlations in promoter methylation and gene expression ($P = 3.0 \times 10^{-3}$, multinomial test; compared to positively correlated/uncorrelated promoter CpGs) (table S7). Two examples, *CHFR* and *MEST*, are presented in fig. S5. These results suggest that dual mechanisms of epigenetic control may regulate these genes, that is, promoter hypermethylation and gene body hypomethylation leading to repression, or promoter hypomethylation and gene body hypermethylation leading to activation. The existence of such "tandem control" mechanisms suggests that promoter DNA methylation alterations may interact with CpG methylation in gene bodies in the same tumors to regulate cancer gene expression (fig. S5).

CIMP cancer subtype identified by genome-wide methylation clustering

Previous studies have proposed that certain gastric cancers may display CpG island methylator phenotype (CIMP) features (*9*, *29*); however, it remains controversial whether CIMP gastric cancers are associated with good or poor prognosis. This might be due to earlier studies relying on restricted sets of molecular markers (for example, *MLH1* and *MINT1*) (*29*) and small patient cohorts (*30*). We investigated whether a gastric CIMP molecular subtype might be identified by genome-wide methylation data. Using methylation levels corresponding to the 1653 expression-associated CpGs, we clustered the 203 tumors using a relative clustering method previously used in methylation array analyses of other tumor types to identify tumor subgroups exhibiting different levels of hyper- and hypomethylation (*13*, *17*). We identified two major tumor clusters: one cluster exhibiting prevalent hypermethylation (CIMP) and another cluster exhibiting relative hypomethylation (Fig. 3A). The hypermethylated tumors exhibited features of gastric CIMP tumors such as *MLH1*, *CDKN2A*, and *MGMT* hypermethylation (*9*, *31*) (Fig. 3A). Similar clustering results were obtained with the top ~5000 CpGs exhibiting the highest across-tumor SDs, and further confirmed by the presence of *CDH1* methylation, another gastric CIMP hallmark (fig. S6) (*32*). Clustering the tumors by their mRNA expression levels did not result in an obvious rediscovery of the CIMP phenotype (fig. S7), suggesting that although large DNA methylation differences are present between CIMP and non-CIMP tumors, the groups are far less obviously discernible by gene expression patterns. It is thus possible that DNA methylation patterns can provide additional discriminatory power to subdivide tumors beyond gene expression levels alone.

We correlated the CIMP status of tumors with several clinicopathologic variables, including survival, age, gender, Epstein-Barr virus (EBV) status, microsatellite instability (MSI) status, grade, stage, and Lauren classification, a traditional histopathological system that classifies gastric cancers into intestinal, diffuse, or "mixed" subtypes (table S8). CIMP tumors tended to be associated with younger patient age, with an average age of 59 compared to 65 ($P = 8 \times 10^{-3}$, Wilcoxon rank sum test), and undifferentiated or poor histologic differentiation ($P = 0.052$, Fisher's exact test). These results support previous studies reporting that global hypomethylation is strongly correlated with age in gastric

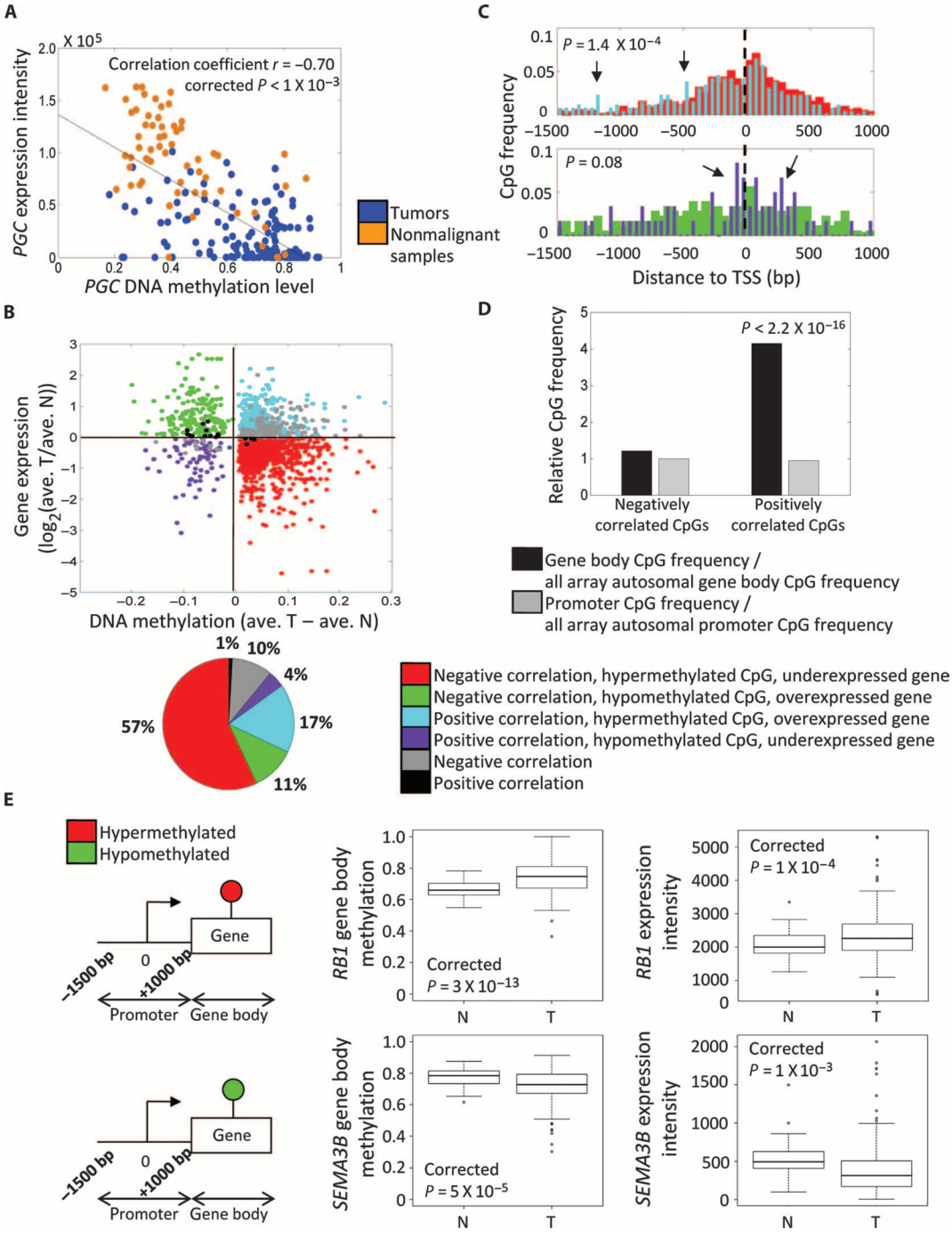

Fig. 2. Impact of methylation alterations on gastric cancer gene expression. (**A**) Example of a gene (*PGC*) exhibiting a negative methylation–gene expression relationship. Blue, tumors; gold, matched controls. (**B**) (Top) Starburst plot of CpG methylation and gene expression differences in tumors and controls. Only CpGs (points) demonstrating significant methylation-expression correlations are shown. *X* axis, methylation differences between tumors and controls. *Y* axis, gene expression differences between tumors and controls. (Bottom) Percentages of significantly correlated CpGs corresponding to the starburst plot. "Underexpressed" and "overexpressed" refer to tumor gene expression. (**C**) Relationships of positively correlated CpG sites to TSSs. (Top) Normalized histogram of positively correlated CpGs exhibiting tumor hypermethylation and overexpression (blue) compared to conventional negatively correlated CpGs (red). (Bottom) Histogram of positively correlated CpGs exhibiting tumor hypomethylation and underexpression (purple) compared to conventional negatively correlated CpGs (green). Black arrows, deviations of positively correlated CpG distributions from negatively correlated CpG distributions. (**D**) Bar graphs showing ratios of gene body (black) and promoter (gray) CpG frequencies within negatively and positively correlated CpGs to all array autosomal gene body and promoter CpG frequencies. *P* values were computed with χ^2 test. (**E**) (Left) Schematic representation of genes containing significantly positively correlated gene body CpGs for *RB1* (top) and *SEMA3B* (bottom). (Middle) Box plots comparing gene body methylation levels of positively correlated gene body CpGs in tumors and nontumor controls. (Right) Box plots comparing expression levels associated with positively correlated gene body CpGs in tumors and nontumor controls.

Table 1. Gene exhibiting altered methylation and expression in gastric cancer.

A. Top hypermethylated and underexpressed genes in gastric cancers with significant negative expression-methylation correlations (corrected $P < 0.05$) (CpGs exhibiting the largest correlation coefficient magnitude for each gene are shown)

Gene name	Difference in gene expression (log_2 ave. T/ave. N)	Difference in DNA methylation (ave. T − ave. N) (range, 0.005–0.33; mean, 0.05)	Correlation coefficient
MT3	−4.38	0.09	−0.22
KCNE2	−4.31	0.17	−0.52
GPR155	−3.40	0.03	−0.20
PSCA	−2.88	0.17	−0.36
LIPF	−2.85	0.06	−0.25
MYRIP	−2.82	0.11	−0.36
KCNJ15	−2.66	0.14	−0.42
MT1G	−2.55	0.03	−0.25
CA9	−2.46	0.08	−0.31
PTGER3	−2.41	0.11	−0.28
PGC	−2.38	0.27	−0.70
GSTA2	−2.36	0.05	−0.26
ADA	−2.33	0.09	−0.35
VSIG2	−2.28	0.08	−0.36
BHLHB8	−2.23	0.04	−0.51
MT1F	−2.19	0.05	−0.22
TFF2	−2.13	0.13	−0.38
SOSTDC1	−2.11	0.05	−0.24
ALDH6A1	−2.07	0.01	−0.18
GCNT2	−2.07	0.15	−0.46

B. Top hypomethylated and overexpressed genes in gastric tumors exhibiting significant negative expression-methylation correlations

Gene name	Difference in gene expression (log_2 ave. T/ave. N)	Difference in DNA methylation (ave. T − ave. N) (range, −0.007 to −0.27; mean, −0.07)	Correlation coefficient
MFAP2	2.68	−0.07	−0.27
H19	2.53	−0.04	−0.50
KRT7	2.38	−0.11	−0.48
KRT17	2.24	−0.10	−0.36
TEAD4	1.88	−0.07	−0.36
MEST	1.70	−0.20	−0.51
HAVCR2	1.67	−0.10	−0.24
FCGR1A	1.61	−0.04	−0.21
TFF3	1.60	−0.09	−0.38
TRIM15	1.59	−0.08	−0.33
CEACAM5	1.53	−0.07	−0.59
NNMT	1.52	−0.08	−0.18
BST2	1.51	−0.12	−0.66
CEACAM6	1.46	−0.08	−0.51
TRIM29	1.39	−0.09	−0.39
RAI14	1.39	−0.09	−0.38
OSMR	1.37	−0.05	−0.23
LIF	1.30	−0.13	−0.28
MMP1	1.28	−0.11	−0.17
CCDC76	1.26	−0.06	−0.27

cancer (*10*). In a survival analysis, patients with CIMP tumors tended to exhibit worse survival outcomes compared to patients with non-CIMP tumors [$P = 0.012$; hazard ratio (HR), 1.641; 95% confidence interval (CI), 1.115 to 2.415] (Fig. 3B). A multivariate analysis confirmed that this difference in patient survival is independent of tumor stage ($P = 0.021$; HR, 1.644; 95% CI, 1.077 to 2.509; table S9).

We explored the biology of the gastric CIMP tumors. GSEA of the top ~2000 CpG sites hypermethylated in CIMP tumors ($P < 0.05$, corrected for multiple testing) revealed that they were enriched in genes related to stem cells [for example, embryonic stem cells (*33*); corrected $P = 3.75 \times 10^{-40}$]. A separate analysis of the ~5000 CpG sites exhibiting high across-tumor variance also confirmed that genes hypermethylated in CIMP tumors exhibited H3K27me3 promoter marks in human embryonic stem cells and were targets of the Polycomb PRC2 complex (*34*) (table S10). These initial observations were confirmed with a more restricted gene set of 316 genes (intersecting the ~2000 and ~5000 CpG sites from the previous analyses) associated with CpG sites differentially methylated between CIMP and non-CIMP groups ($P < 0.05$, Bonferroni correction), indicating that they are not simply due to the use of a large gene set (table S10). This finding suggests that genes hypermethylated in gastric CIMP tumors may be related to Polycomb targets in stem cells. Taken collectively, these results suggest that CIMP tumors may represent a clinically and biologically distinct subgroup of gastric cancers.

Sensitivity of gastric CIMP cell lines to DNA methylation inhibitors

5-Aza-2′-deoxycytidine (5-Aza-dC) is a DNA methyltransferase inhibitor approved for human use in myelodysplastic syndrome (*35*). To test whether gastric CIMP tumors might be sensitive to 5-Aza-dC,

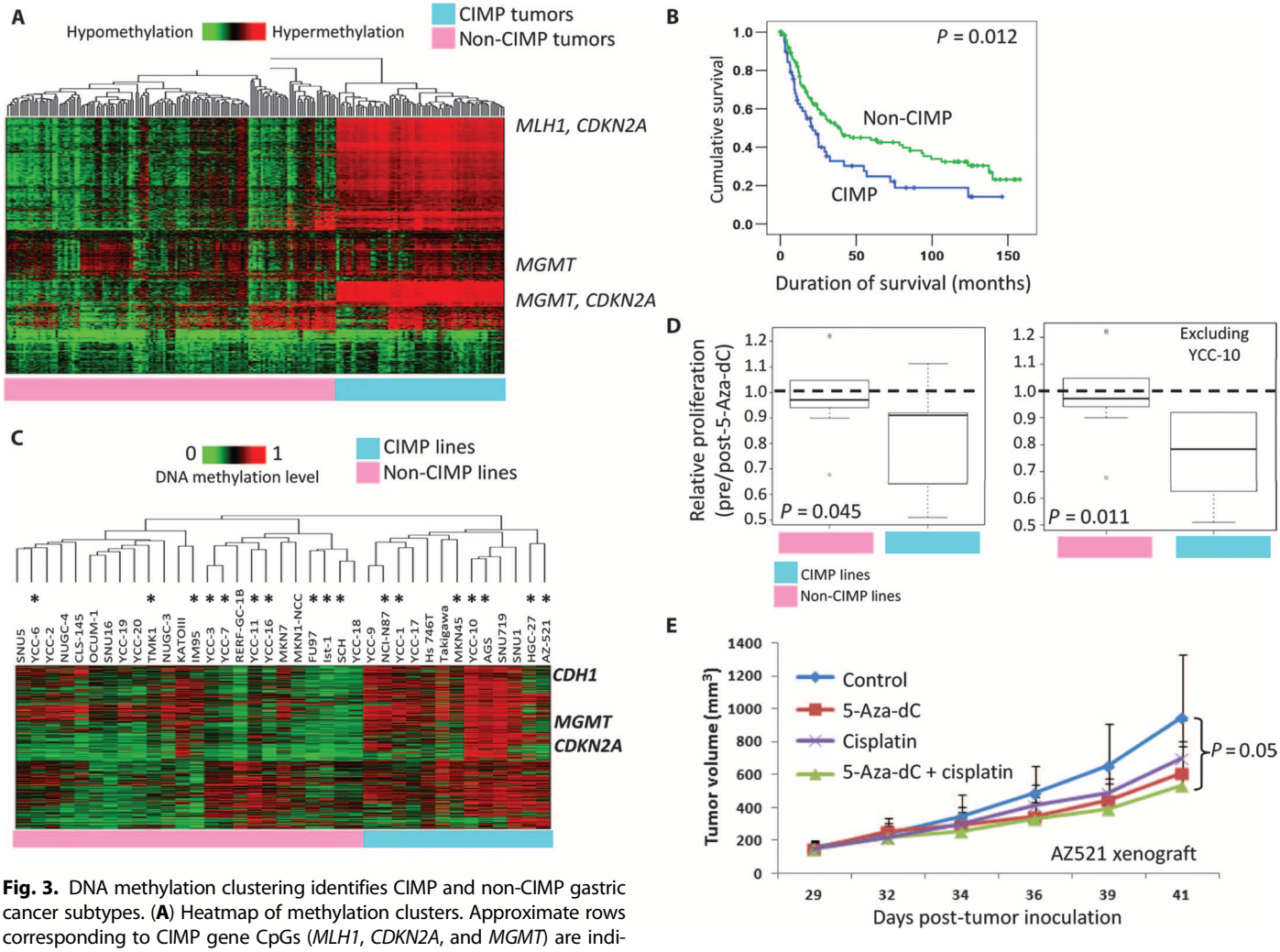

Fig. 3. DNA methylation clustering identifies CIMP and non-CIMP gastric cancer subtypes. (**A**) Heatmap of methylation clusters. Approximate rows corresponding to CIMP gene CpGs (*MLH1*, *CDKN2A*, and *MGMT*) are indicated. CIMP and non-CIMP tumors are indicated by blue and pink bars, respectively. (**B**) Kaplan-Meier overall survival plot comparing CIMP and non-CIMP patients. (**C**) Heatmap of gastric cancer cell lines clustered by DNA methylation data. Approximate rows corresponding to *CDH1*, *CDKN2A*, and *MGMT* CpGs are indicated. Asterisk, cell lines used in drug treatment experiments. (**D**) Cellular responses of CIMP and non-CIMP lines to 5-Aza-dC. (Left) Relative proliferation (pre/post–5-Aza-dC) for CIMP and non-CIMP cell lines. The dashed horizontal line (value 1) represents no change after 5-Aza-dC treatment. (Right) Relative proliferation (pre/post–5-Aza-dC) for CIMP and non-CIMP lines after removal of one cell line (YCC-10). *P* values were computed with two-sided Mann-Whitney tests. (**E**) Murine xenograft assays of AZ521 CIMP cells. Treatment groups were control, cisplatin, 5-Aza-dC, and cisplatin/5-Aza-dC combined. Comparisons were performed between control and drug treatment groups with Student's *t* test.

we identified in vitro CIMP cell line models. Clustering the cell lines by their global methylation profiles, we identified CIMP lines exhibiting widespread high DNA methylation levels, and *CDH1*, *MGMT*, and *CDKN2A* hypermethylation (Fig. 3C). We treated 7 CIMP lines (YCC-10, MKN45, AZ-521, NCI-N87, AGS, HGC-27, and YCC-1) and 10 non-CIMP lines (Ist-1, SCH, YCC-16, TMK1, YCC-11, YCC-3, IM95, YCC-6, YCC-7, and FU97) with 5-Aza-dC at experimental dosages and time periods previously used (5 μM, 72 hours) (*36*). Non-CIMP cell lines exhibited little or no changes in proliferation after 5-Aza-dC treatment (average proliferation change = 0.99). However, CIMP lines exhibited significant reductions in proliferation after treatment (average relative proliferation = 0.81) ($P = 0.045$, Wilcoxon rank sum test) (Fig. 3D). Removal of one outlier CIMP cell line (YCC-10) from this analysis confirmed an even stronger difference in proliferation after 5-Aza-dC treatment ($P = 0.011$, Wilcoxon rank sum test) (Fig. 3D). To test the efficacy of 5-Aza-dC in an in vivo context, we conducted murine xenograft experiments, where the growth of CIMP-positive AZ521 cells was monitored after treatment with control, cisplatin, 5-Aza-dC, or a cisplatin/5-Aza-dC combination. Significant reductions in tumor growth were observed in the cisplatin/5-Aza-dC–treated group relative to controls ($P = 0.05$; Fig. 3E). These results suggest that gastric CIMP tumors may be sensitive to 5-Aza-dC therapy, potentially in combination with standard chemotherapies.

LRESs and expression regulation in gastric CIMP tumors

LRESs are large chromosomal regions hypermethylated in cancer (*15*). To identify LRESs in gastric cancer, we implemented a sliding window algorithm to identify genomic regions exhibiting significant enrichments of hypermethylated CpGs in tumors relative to normals compared to other regions in the genome. Using this approach, we identified seven potential LRESs (table S11). DNA methylation levels at CpG sites in these genomic regions exhibited significantly higher correlation to one another compared to other randomly selected genomic regions of similar length, gene, and CpG density ($P = 0.01$, Wilcoxon rank sum test) (Fig. 4A). The presence of these LRESs was significantly associated with CIMP status ($P = 3.7 \times 10^{-15}$, χ^2 test) (Fig. 4B and table S12). An analysis of genes in the LRESs revealed several regions plausibly related to cancer. For example, LRES1, which is located at 2q31.1 (1.90 Mb), comprises the *HOXD* cluster, a known hotspot of concerted de novo methylation in cancer (*37*).

To characterize the methylation structure of a specific LRES in greater detail, we analyzed LRES5, a 1.5-Mb region on chromosome 11 containing six genes. Using newer-generation Illumina 450K methylation arrays, we measured fine-scale methylation patterns in LRES5 from four CIMP tumor/normal pairs across 411 CpG probes. Fifty-nine percent of the LRES5 CpG probes exhibited cancer-specific hypermethylation, significantly greater than the genome background in these same tumors ($P = 0.038$). Cancer-specific hypermethylation in LRES5 was particularly focused around CGIs and CGI shores ($P = 0.00032$, χ^2 test) but not in intergenic regions (fig. S8).

LRESs might act to regulate all genes within the LRES or only specific LRES genes. Tumors with LRES5 hypermethylation exhibited lower levels of LRES5-specific gene expression compared to tumors with minimal LRES5 methylation ($P = 8.1 \times 10^{-3}$, two-sided t test) (Fig. 4C). However, among the LRES5 genes, *ALKBH3* exhibited the strongest and most consistent negative methylation-expression correlations to the LRES5 CpGs (Fig. 4D; $P = 2.5 \times 10^{-9}$, Kruskal-Wallis test) even to LRES5 CpGs localized distantly to *ALKBH3* (Fig. 4E and table S13). A permutation analysis revealed that this frequency was unlikely to occur by random chance [false discovery rate (FDR) = 0.37%]. To test whether *ALKBH3* might represent the primary gene silenced in LRES5, we identified two CIMP lines exhibiting LRES5 hypermethylation and underexpression (NCI-N87 and YCC-10). Treating these lines with 5-Aza-dC induced *ALKBH3* overexpression to nearly four- and twofold levels, respectively (Fig. 4F). In contrast, *PHACS*, another LRES5 gene, was not overexpressed upon 5-Aza-dC treatment (Fig. 4F). These results suggest that in some cases, LRESs may target and silence specific genes, rather than all genes within the region.

Similarly, LRES3 analysis revealed that *COMMD3* is the most likely target of methylation alterations in LRES3. *COMMD3* exhibited the strongest negative methylation-expression correlations among the five LRES3 genes ($P = 0.015$, Kruskal-Wallis test; Fig. 4D) and was also negatively correlated with the highest number of CpGs spanning LRES3 (Fig. 4E and table S14). 5-Aza-dC treatment of AGS cells, which are CIMP-positive and exhibit LRES3 hypermethylation, resulted in statistically significant overexpression of *COMMD3* but not other LRES3 genes ($P = 0.01$; Fig. 4F). These results suggest that for certain LRESs, coordinated CpG methylation may act over large genomic distances to target and alter the expression of specific genes.

Long-range regions of hypomethylation and genomic instability

Finally, our initial observation of tumor hypomethylation (Fig. 1) prompted us to investigate the potential existence of long-range regions of tumor-specific hypomethylation (that is, reduced methylation). Using a sliding window approach similar to the one used to identify the LRESs, we discovered 24 regions of long-range hypomethylation (hypo-LRRs) (table S15). The average degree of hypomethylation in the 24 hypo-LRRs regions was 0.03 (β = 0.01 to 0.04), consistent with the hypo-LRR regions exhibiting subtle but consistent patterns of tumor-associated hypomethylation. Similar to the LRESs, hypo-LRRs exhibited higher levels of coordinated methylation relative to the rest of the genome, with greater numbers of CpG-CpG methylation correlations compared to other regions of the genome of comparable length and gene density ($P = 6.2 \times 10^{-14}$, Wilcoxon rank sum test) (fig. S9). The hypo-LRRs were significantly longer than LRESs (average, 1.8 versus 1.34 Mb) and harbored more genes (average, 53 versus 8 genes) ($P = 0.047$ and 7.9×10^{-5}, respectively; Wilcoxon rank sum test). Hypo-LRRs also occurred predominantly in non-CIMP tumors ($P = 0.02$, χ^2 test) (fig. S9 and table S16). We investigated whether the hypo-LRRs might be associated with the presence of repeat sequences by comparing them against nine different sequence repeat classes. Of the 24 hypo-LRRs regions, only one hypo-LRR (region 6 on chromosome 11) exhibited a significant enrichment in repeat sequences ($P = 0.04$, compared to 1000 randomly selected regions of similar length) (table S17). There thus does not seem to be an obvious association between the hypo-LRRs and repeat sequences.

Hypomethylation can induce chromosome breakage events. The availability of high-density copy number data for this same gastric cancer cohort (*38*) allowed us to directly test for any association between hypo-LRRs and genome instability. Specifically, we tested whether tumors exhibiting specific hypo-LRRs were also prone to genome instability in those same regions. Strikingly, we found that most of hypo-LRRs were indeed significantly associated with increased genome instability ($P = 6.0 \times 10^{-6}$; Fig. 5). The association between hypo-LRR presence and genome instability was also observed at the level of individual hypo-LRRs (fig. S10).

DISCUSSION

This study reports a genome-wide survey of the gastric cancer DNA methylation landscape. Our results are limited to those CpGs present on the Infinium 27K methylation array, which are focused toward promoter regions and CGIs. We are unable to comment on methylation patterns in intragenic regions and gene deserts, which are better represented by other platforms [for example, 450K methylation array and whole-genome bisulfite sequencing (*39*)]. This caveat notwithstanding, for regions well interrogated by the 27K array, our results are likely to be robust, being based on a large sample series and rigorous statistical analysis. We found that gastric cancer–associated DNA methylation alterations were widespread, with most tumor-associated CpGs (83%) hypermethylated in gastric cancers and tending to localize at CGIs. However, we also observed significant cancer-specific CpG hypomethylation. A recent whole-genome bisulfite sequencing study of a CIMP colon cancer (*39*) has also similarly reported that tumor-specific hypermethylation is restricted to CGIs, and that tumors appear to exhibit a greater extent of absolute hypomethylation than hypermethylation ($P < 2.2 \times 10^{-16}$, Wilcoxon rank sum test; in our study).

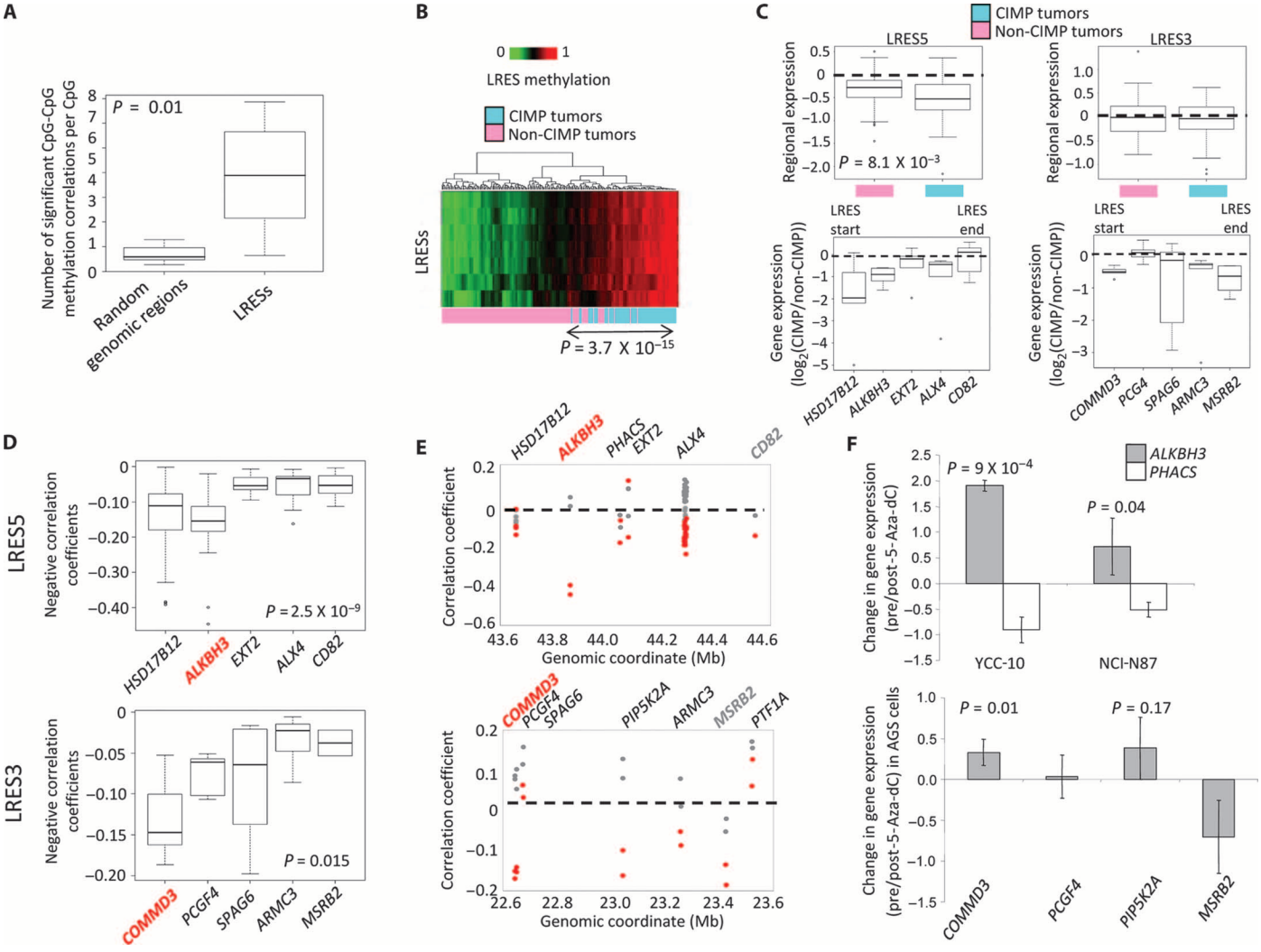

Fig. 4. LRESs in gastric CIMP tumors. (**A**) Box plots showing significant CpG-CpG methylation correlations per CpG for LRESs or random genomic regions. *P* value was computed by a two-sided Mann-Whitney test. (**B**) Heatmap of gastric tumors clustered by LRES methylation. Color bars represent the extent of LRES hypermethylation. (**C**) Regional LRES expression in CIMP and non-CIMP tumors. (Left) LRES5. (Right) LRES3. (Top) Regional expression of LRES5 or LRES3 genes in CIMP and non-CIMP tumors. (Bottom) Gene expression levels (Affymetrix) of individual LRES genes between CIMP and non-CIMP tumors. CIMP tumors with LRES methylation levels >0.9 exhibited lower regional expression levels than non-CIMP tumors with LRES methylation levels <0.3. (**D**) Box plot of correlation coefficients for all LRES CpGs against each LRES gene with Affymetrix expression data. (Top) LRES5. (Bottom) LRES3. (**E**) Correlation coefficients for all LRES5 and LRES3 CpG methylation levels correlated to *ALKBH3* and *COMMD3* expression, respectively, with respect to genomic coordinate. Plots of other representative LRES genes are provided for comparison (*CD82* and *MSRB2*). (**F**) Gene expression differences for LRES5 and LRES3 genes with Illumina expression data are shown after 5-Aza-dC treatment. Gastric tumor cell lines displaying LRES5 and LRES3 hypermethylation were treated. Expression differences are the $\log_2$-transformed ratio of the mean expression intensity of the 5-Aza-dC–treated cells to that of the untreated cells. *P* values were calculated by two-sided *t* tests. Error bars, SD over three biological replicates.

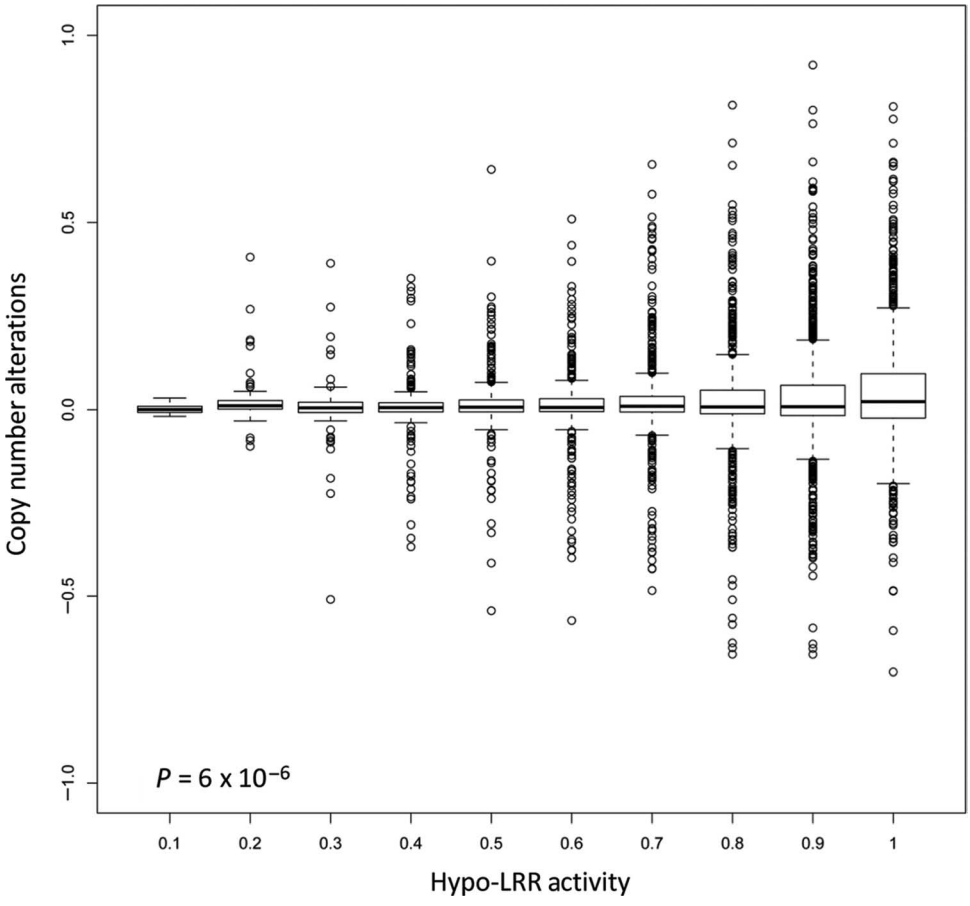

Fig. 5. Copy number alterations (CNAs) and hypo-LRRs. The box plot presents data from 24 hypo-LRRs across 190 gastric cancers with methylation and copy number information. Each dot represents one hypo-LRR in one tumor. *X* axis, level of hypo-activity from 0 to 1, marking increasing hypomethylation from left to right. *Y* axis, CNA level, represented by the LRR (log relative ratio). *P* values were calculated with a correlation test of SD between CNA LRR and hypo-LRR activity.

Integrating the methylation data with transcriptional information, we found that ~25% of CpG sites exhibited significant correlations with gene expression. This value should be treated with caution because transcription levels for certain genes may be differentially correlated to CpG methylation at one site compared to other adjacent sites (*40*) and, as previously stated, the 27K Infinium methylation array does not comprehensively interrogate all CpGs. Although most of the methylation-expression relationships were negative (78%), we also observed a significant number of positive methylation-expression relationships (22%). Analysis of these positively correlated CpGs revealed that these were associated with distinct sequence and gene features and also tended to occur within gene bodies. Although previous studies have reported that DNA methylation at nucleosome-free regions at TSSs is causally involved in gene silencing (*41*) and that gene body methylation is associated with increased gene expression (*42*, *43*), many of these earlier studies were based largely on in vitro systems (for example, cell lines) or on very few primary samples [for example, a single B cell sample in (*43*)]. In this regard, our study provides value in confirming the presence of such correlations between DNA methylation and gene expression in a large series of primary human tissues.

In our series, we identified 220 promoters with opposing methylation effects, whereas Kobayashi *et al.* identified 223 in a recent prostate cancer study (*17*). Within these promoters, hypomethylated CpGs tended to lie farther away from the TSS than hypermethylated CpGs (136 of 218 CpGs; $P = 2.5 \times 10^{-4}$, χ^2 test), and hypomethylated CpGs in these promoters tended to lie upstream of TSSs, whereas hypermethylated CpGs tended to lie downstream of TSSs ($P = 3.21 \times 10^{-6}$, Wilcoxon rank sum test). The median CpG-TSS distances for hypermethylated and hypomethylated CpGs in our series were 43 and −342 bp, respectively, comparable to the corresponding ranges of CpG-TSS distances reported by Kobayashi *et al.* (−100 to +800 and −700 to −200, respectively). These shared patterns suggest that some of the epigenetic patterns observed in gastric cancer may also apply to other tumor types.

Our study demonstrates the gastric CIMP phenotype on a genome-wide scale. Although previously proposed (*9*, *29*), CIMP status is currently not routinely assessed in gastric cancer diagnosis. Moreover, whereas some have reported that gastric CIMP tumors are associated with good prognosis (*30*, *44*), others have observed an association with poor prognosis (*11*, *45*). It is possible that these clinical differences might be influenced by the specific panel of methylation markers chosen for measurement and by the relatively small sizes of these earlier studies. In our study, we confirmed that gastric CIMP tumors indeed exhibited widespread genome-wide patterns (>1000 CpG sites) of hypermethylation, and that gastric cancer patients with CIMP tumors tended to be younger and have a decreased survival rate, even after adjusting for disease stage. Intriguingly, at the molecular level, genes methylated in CIMP tumors appeared to show overlap with targets of Polycomb group proteins in embryonic stem cells. This finding suggests that the widespread hypermethylation found in gastric CIMP tumors may be related to the activity of Polycomb group proteins, which can alter chromatin structure, control gene silencing, and induce de novo methylation (*9*, *46*).

We found that CIMP cell lines exhibited significantly greater cell proliferation reductions in response to 5-Aza-dC (decitabine) compared to non-CIMP lines. In colorectal cancers, CIMP tumors have been reported to exhibit increased sensitivity to adjuvant chemotherapy (*47*). Our results represent an example of a CIMP cancer exhibiting increased cellular sensitivity to a DNA methylation inhibitor. Although the differences between the CIMP and non-CIMP lines are admittedly subtle in absolute terms, we believe that this is a noteworthy finding, particularly because 5-Aza-dC is already clinically approved for use in human myelodysplastic syndrome. We also found that when the

5-Aza-dC treatments were repeated at a lower concentration (1 μM) on four CIMP and four non-CIMP lines, cell proliferation inhibition was only observed in two of the four CIMP lines (relative proliferation before/after 5-Aza-dC treatment being 0.95 and 0.67 for MKN45 and AZ521, respectively) and none of the non-CIMP cell lines (Y.Z., personal communication). Hence, it is possible that the cell proliferation inhibition caused by 5-Aza-dC in CIMP lines is not only due to DNA demethylation but also may involve other mechanisms such as p53 pathway activation.

Finally, our analysis identified the presence of multiple LRESs (*15*) in CIMP tumors. An analysis of individual LRESs suggests that in addition to generalized regional silencing, in certain LRESs, coordinated epigenetic alterations may target a single gene within the region. *ALKBH3* and *COMMD3*, the putative targets of LRES5 and LRES3 hypermethylation, respectively, have plausible relationships to cancer (*48*, *49*). Given that most methylation events may not play a causative role in tumorigenesis (that is, "passenger methylation") (*50*), these results suggest that considering the effects of DNA methylation over large genomic distances may help to identify genes that are the targets of "driver methylation."

We close our survey of the gastric cancer methylome by noting that *Helicobacter pylori* infection has been shown to induce de novo methylation patterns in nonmalignant gastric mucosae (*51*), associated with "epigenetic field cancerization" and gastric cancer development (*51*). Hence, the gastric cancer epigenetic landscape presented in this study should contribute to our understanding of how environmental (for example, *H. pylori*) and biological perturbations (for example, inflammation) can affect the genomes of gastric epithelial cells to enhance carcinogenic risk.

MATERIALS AND METHODS

Genomic methylation profiling

Genomic DNA from primary gastric tissues and cell lines (*38*) was profiled on Infinium 27K methylation arrays. Methylation analysis with Infinium 450K arrays was also performed on selected CIMP tumors and matched normals. DNA methylation levels for each CpG site were computed by Genome Studio software as the ratio of methylated signal intensity to the sum of methylated and unmethylated signal intensities. The methylation array data have been deposited into the Gene Expression Omnibus (GEO) under accession number GSE30601.

Gene expression profiling and copy number alterations

Gene expression array data are available at the GEO under accession number GSE15460 (*20*). To identify epigenetically silenced genes, we hybridized RNA from control and 5-Aza-dC–treated lines to Illumina Human WG-6 Beadchips (Illumina). Copy number alterations analyzed are available under accession number GSE31168 (*38*). Segmentation was performed with circular binary segmentation (*52*).

CpG methylation and gene expression data analysis

Differential CpG methylation analyses were performed between two groups of samples with two-sided *t* tests, and *P* values were Bonferroni-corrected. Similar methods were used for differential expression analyses, with *P* values corrected with the Benjamini and Hochberg method (*53*). Correlation analyses were performed by calculating Pearson correlation coefficients and *P* values, corrected with the Benjamini and Hochberg method (*53*). Corrected *P* values of <0.05 were considered significant.

Clustering and pathway analysis

Unsupervised hierarchical clustering was performed with a Euclidean distance metric and complete linkage clustering. Before clustering, the tumor methylation data were subjected to a $\log_2$ transformation relative to the mean of the corresponding nonmalignant sample probe. GSEA (*23*) was performed with Molecular Signatures Database version 2.5.1 (http://www.broadinstitute.org/gsea/msigdb/index.jsp). Nominal overlap *P* values were Bonferroni-corrected. Corrected *P* values of <0.05 were considered significant.

Clinicopathologic associations and statistical analysis

Clinical associations between gastric cancer molecular subtypes and gender, tumor grade, Lauren classification, EBV status, MSI status, and disease stage were evaluated with Fisher's exact test. Association with patient age was determined with the Wilcoxon rank sum test. *P* values of <0.05 were considered significant. Kaplan-Meier analysis (SPSS) was performed to compare survival outcomes. Cox regression models were used for computing HRs in univariate and multivariate analyses. Multivariate models were generated only with factors found significant in univariate analysis. Associations of LRESs to CIMP status were calculated with χ^2 tests (one degree of freedom). Associations between non-CIMP tumors and amplified regions were performed with Fisher's exact test. *P* values were corrected with the Benjamini and Hochberg method (*53*). Corrected *P* values of <0.05 were considered significant.

LRES and hypo-LRR analysis

LRES and hypo-LRRs were detected with a 1-Mb sliding window shifted along the genomic coordinate in 50-kb increments. Windows exhibiting a greater (lesser)-than-expected fraction of hyper (hypo)-methylated CpGs were identified by comparison to a null distribution of randomly selected windows of comparable genomic length, and overlapping significant windows were grouped in single LRESs/hypo-LRRs. An FDR cutoff of <10% was used. Regional gene expression values for each LRES in each tumor were computed by $\log_2$ transforming expression values of each LRES gene in each tumor relative to the mean expression level of the same gene in nonmalignant samples and averaging the transformed values within the LRES.

Drug treatments and murine xenograft assays

Cell lines were treated with 5-Aza-dC (5 μM) for 72 hours. Proliferation measurements were determined with a tetrazolium compound–based colorimetric method (MTS kit, Promega) on an EnVision 2104 multilabel plate reader (PerkinElmer). All drug treatment and expression array profiles were performed in triplicate for each cell line. Animal studies were performed in compliance with Institutional Animal Care and Use Committee policies at Van Andel Research Institute. Six-week-old female BALB/c nu/nu nude mice (Charles River) were injected subcutaneously with 2×10^6 AZ521 cells in the right flank. Tumor growth was measured three times per week with digital calipers (Mitutoyo), and tumor volume was calculated as length × width × height × 0.5. Drug treatments were initiated once the tumors grew to 200 to 250 mm^3.

Additional details are provided in the Supplementary Materials.

SUPPLEMENTARY MATERIALS

www.sciencetranslationalmedicine.org/cgi/content/full/4/156/156ra140/DC1
Materials and Methods
Fig. S1. Correlation between Infinium and GoldenGate methylation profiles.
Fig. S2. Unsupervised clustering of gastric tumors and nonmalignant gastric normals using DNA methylation patterns.
Fig. S3. Intersection of genes with DNA methylation and gene expression information.
Fig. S4. Overlap of H3K27ac and H3K4me3 ChIP-Seq binding peaks with CpG sites exhibiting tumor hypermethylation and increased expression.
Fig. S5. Tandem gene body and promoter methylation alterations in genes.
Fig. S6. Clustering of tumor samples based on DNA methylation data.
Fig. S7. Clustering of gastric cancers by gene expression or DNA methylation.
Fig. S8. High-resolution methylation patterns in LRES5.
Fig. S9. Hypo-LRRs: long-range regions (LRRs) of hypomethylation.
Fig. S10. Box plots relating copy number alterations (CNAs) with individual hypomethylated regions (hypo-LRRs 1 to 24).
Table S1. Clinical characteristics of gastric cancer patients analyzed in this study.
Table S2. Correlation between Infinium and GoldenGate methylation.
Table S3. GSEA of hypermethylated genes underexpressed in tumors.
Table S4. GSEA of hypomethylated genes overexpressed in tumors.
Table S5. Association of positively correlated CpGs to H3K27ac and H3K4me3 peaks.
Table S6. Genes exhibiting correlations between gene body methylation and expression.
Table S7. Genes exhibiting tandem promoter and gene body methylation.
Table S8. Clinicopathologic associations of CIMP and non-CIMP tumors.
Table S9. Multivariate analysis of survival associations of CIMP tumors.
Table S10. GSEA of genes hypermethylated in CIMP gastric tumors.
Table S11. LRESs in CIMP gastric cancers.
Table S12. Association of LRESs with CIMP gastric tumors.
Table S13. CpG methylation correlation coefficients with respect to expression of genes within LRES5.
Table S14. CpG methylation correlation coefficients with respect to expression of genes within LRES3.
Table S15. Hypo-LRRs: long-range regions of hypomethylation.
Table S16. Association of hypo-LRRs to non-CIMP tumors.
Table S17. Hypo-LRR CpGs and repeat sequences.

REFERENCES AND NOTES

1. H. Brenner, D. Rothenbacher, V. Arndt, Epidemiology of stomach cancer. *Methods Mol. Biol.* **472**, 467–477 (2009).
2. S. S. Wöhrer, M. Raderer, M. Hejna, Palliative chemotherapy for advanced gastric cancer. *Ann. Oncol.* **15**, 1585–1595 (2004).
3. W. K. Leung, M. S. Wu, Y. Kakugawa, J. J. Kim, K. G. Yeoh, K. L. Goh, K. C. Wu, D. C. Wu, J. Sollano, U. Kachintorn, T. Gotoda, J. T. Lin, W. C. You, E. K. Ng, J. J. Sung; Asia Pacific Working Group on Gastric Cancer, Screening for gastric cancer in Asia: Current evidence and practice. *Lancet Oncol.* **9**, 279–287 (2008).
4. H. H. Hartgrink, E. P. Jansen, N. C. van Grieken, C. J. van de Velde, Gastric cancer. *Lancet* **374**, 477–490 (2009).
5. J. G. Strickler, J. Zheng, Q. Shu, L. J. Burgart, S. R. Alberts, D. Shibata, *p53* mutations and microsatellite instability in sporadic gastric cancer: When guardians fail. *Cancer Res.* **54**, 4750–4755 (1994).
6. Y. Kimura, T. Noguchi, K. Kawahara, K. Kashima, T. Daa, S. Yokoyama, Genetic alterations in 102 primary gastric cancers by comparative genomic hybridization: Gain of 20q and loss of 18q are associated with tumor progression. *Mod. Pathol.* **17**, 1328–1337 (2004).
7. P. A. Jones, S. B. Baylin, The epigenomics of cancer. *Cell* **128**, 683–692 (2007).
8. A. P. Feinberg, B. Vogelstein, Hypomethylation distinguishes genes of some human cancers from their normal counterparts. *Nature* **301**, 89–92 (1983).
9. M. Toyota, N. Ahuja, H. Suzuki, F. Itoh, M. Ohe-Toyota, K. Imai, S. B. Baylin, J. P. Issa, Aberrant methylation in gastric cancer associated with the CpG island methylator phenotype. *Cancer Res.* **59**, 5438–5442 (1999).
10. K. Suzuki, I. Suzuki, A. Leodolter, S. Alonso, S. Horiuchi, K. Yamashita, M. Perucho, Global DNA demethylation in gastrointestinal cancer is age dependent and precedes genomic damage. *Cancer Cell* **9**, 199–207 (2006).
11. S. Y. Park, M. C. Kook, Y. W. Kim, N. Y. Cho, N. Jung, H. J. Kwon, T. Y. Kim, G. H. Kang, CpG island hypermethylator phenotype in gastric carcinoma and its clinicopathological features. *Virchows Arch.* **457**, 415–422 (2010).
12. M. E. Figueroa, S. Lugthart, Y. Li, C. Erpelinck-Verschueren, X. Deng, P. J. Christos, E. Schifano, J. Booth, W. van Putten, L. Skrabanek, F. Campagne, M. Mazumdar, J. M. Greally, P. J. Valk, B. Löwenberg, R. Delwel, A. Melnick, DNA methylation signatures identify biologically distinct subtypes in acute myeloid leukemia. *Cancer Cell* **17**, 13–27 (2010).
13. H. Noushmehr, D. J. Weisenberger, K. Diefes, H. S. Phillips, K. Pujara, B. P. Berman, F. Pan, C. E. Pelloski, E. P. Sulman, K. P. Bhat, R. G. Verhaak, K. A. Hoadley, D. N. Hayes, C. M. Perou, H. K. Schmidt, L. Ding, R. K. Wilson, D. Van Den Berg, H. Shen, H. Bengtsson, P. Neuvial, L. M. Cope, J. Buckley, J. G. Herman, S. B. Baylin, P. W. Laird, K. Aldape; Cancer Genome Atlas Research Network, Identification of a CpG island methylator phenotype that defines a distinct subgroup of glioma. *Cancer Cell* **17**, 510–522 (2010).
14. R. A. Irizarry, C. Ladd-Acosta, B. Wen, Z. Wu, C. Montano, P. Onyango, H. Cui, K. Gabo, M. Rongione, M. Webster, H. Ji, J. B. Potash, S. Sabunciyan, A. P. Feinberg, The human colon cancer methylome shows similar hypo- and hypermethylation at conserved tissue-specific CpG island shores. *Nat. Genet.* **41**, 178–186 (2009).
15. M. W. Coolen, C. Stirzaker, J. Z. Song, A. L. Statham, Z. Kassir, C. S. Moreno, A. N. Young, V. Varma, T. P. Speed, M. Cowley, P. Lacaze, W. Kaplan, M. D. Robinson, S. J. Clark, Consolidation of the cancer genome into domains of repressive chromatin by long-range epigenetic silencing (LRES) reduces transcriptional plasticity. *Nat. Cell Biol.* **12**, 235–246 (2010).
16. M. Bibikova, J. Le, B. Barnes, S. Saedinia-Melnyk, L. Zhou, R. Shen, K. L. Gunderson, Genome-wide DNA methylation profiling using Infinium assay. *Epigenomics* **1**, 177–200 (2009).
17. Y. Kobayashi, D. M. Absher, Z. G. Gulzar, S. R. Young, J. K. McKenney, D. M. Peehl, J. D. Brooks, R. M. Myers, G. Sherlock, DNA methylation profiling reveals novel biomarkers and important roles for DNA methyltransferases in prostate cancer. *Genome Res.* **21**, 1017–1027 (2011).
18. T. Hinoue, D. J. Weisenberger, C. P. Lange, H. Shen, H. M. Byun, D. Van Den Berg, S. Malik, F. Pan, H. Noushmehr, C. M. van Dijk, R. A. Tollenaar, P. W. Laird, Genome-scale analysis of aberrant DNA methylation in colorectal cancer. *Genome Res.* **22**, 271–282 (2012).
19. F. Eckhardt, J. Lewin, R. Cortese, V. K. Rakyan, J. Attwood, M. Burger, J. Burton, T. V. Cox, R. Davies, T. A. Down, C. Haefliger, R. Horton, K. Howe, D. K. Jackson, J. Kunde, C. Koenig, J. Liddle, D. Niblett, T. Otto, R. Pettett, S. Seemann, C. Thompson, T. West, J. Rogers, A. Olek, K. Berlin, S. Beck, DNA methylation profiling of human chromosomes 6, 20 and 22. *Nat. Genet.* **38**, 1378–1385 (2006).
20. C. H. Ooi, T. Ivanova, J. Wu, M. Lee, I. B. Tan, J. Tao, L. Ward, J. H. Koo, V. Gopalakrishnan, Y. Zhu, L. L. Cheng, J. Lee, S. Y. Rha, H. C. Chung, K. Ganesan, J. So, K. C. Soo, D. Lim, W. H. Chan, W. K. Wong, D. Bowtell, K. G. Yeoh, H. Grabsch, A. Boussioutas, P. Tan, Oncogenic pathway combinations predict clinical prognosis in gastric cancer. *PLoS Genet.* **5**, e1000676 (2009).
21. D. Deng, W. El-Rifai, J. Ji, B. Zhu, P. Trampont, J. Li, M. F. Smith, S. M. Powel, Hypermethylation of metallothionein-3 CpG island in gastric carcinoma. *Carcinogenesis* **24**, 25–29 (2003).
22. Study Group of Millennium Genome Project for Cancer; H. Sakamoto, K. Yoshimura, N. Saeki, H. Katai, T. Shimoda, Y. Matsuno, D. Saito, H. Sugimura, F. Tanioka, S. Kato, N. Matsukura, N. Matsuda, T. Nakamura, I. Hyodo, T. Nishina, W. Yasui, H. Hirose, M. Hayashi, E. Toshiro, S. Ohnami, A. Sekine, Y. Sato, H. Totsuka, M. Ando, R. Takemura, Y. Takahashi, M. Ohdaira, K. Aoki, I. Honmyo, S. Chiku, K. Aoyagi, H. Sasaki, S. Ohnami, K. Yanagihara, K. A. Yoon, M. C. Kook, Y. S. Lee, S. R. Park, C. G. Kim, I. J. Choi, T. Yoshida, Y. Nakamura, S. Hirohashi, Genetic variation in *PSCA* is associated with susceptibility to diffuse-type gastric cancer. *Nat. Genet.* **40**, 730–740 (2008).
23. A. Subramanian, P. Tamayo, V. K. Mootha, S. Mukherjee, B. L. Ebert, M. A. Gillette, A. Paulovich, S. L. Pomeroy, T. R. Golub, E. S. Lander, J. P. Mesirov, Gene set enrichment analysis: A knowledge-based approach for interpreting genome-wide expression profiles. *Proc. Natl. Acad. Sci. U.S.A.* **102**, 15545–15550 (2005).
24. V. K. Mootha, C. M. Lindgren, K. F. Eriksson, A. Subramanian, S. Sihag, J. Lehar, P. Puigserver, E. Carlsson, M. Ridderstråle, E. Laurila, N. Houstis, M. J. Daly, N. Patterson, J. P. Mesirov, T. R. Golub, P. Tamayo, B. Spiegelman, E. S. Lander, J. N. Hirschhorn, D. Altshuler, L. C. Groop, PGC-1α-responsive genes involved in oxidative phosphorylation are coordinately downregulated in human diabetes. *Nat. Genet.* **34**, 267–273 (2003).
25. M. Vecchi, P. Nuciforo, S. Romagnoli, S. Confalonieri, C. Pellegrini, G. Serio, M. Quarto, M. Capra, G. C. Roviaro, E. Contessini Avesani, C. Corsi, G. Coggi, P. P. Di Fiore, S. Bosari, Gene expression analysis of early and advanced gastric cancers. *Oncogene* **26**, 4284–4294 (2007).
26. Y. Wu, M. S. Siadaty, M. E. Berens, G. M. Hampton, D. Theodorescu, Overlapping gene expression profiles of cell migration and tumor invasion in human bladder cancer identify metallothionein 1E and nicotinamide N-methyltransferase as novel regulators of cell migration. *Oncogene* **27**, 6679–6689 (2008).
27. S. Senese, K. Zaragoza, S. Minardi, I. Muradore, S. Ronzoni, A. Passafaro, L. Bernard, G. F. Draetta, M. Alcalay, C. Seiser, S. Chiocca, Role for histone deacetylase 1 in human tumor cell proliferation. *Mol. Cell. Biol.* **27**, 4784–4795 (2007).
28. M. Nuytten, L. Beke, A. Van Eynde, H. Ceulemans, M. Beullens, P. Van Hummelen, F. Fuks, M. Bollen, The transcriptional repressor NIPP1 is an essential player in EZH2-mediated gene silencing. *Oncogene* **27**, 1449–1460 (2008).
29. B. Carvalho, M. Pinto, L. Cirnes, C. Oliveira, J. C. Machado, G. Suriano, R. Hamelin, F. Carneiro, R. Seruca, Concurrent hypermethylation of gene promoters is associated with a MSI-H phenotype and diploidy in gastric carcinomas. *Eur. J. Cancer* **39**, 1222–1227 (2003).

30. C. An, I. S. Choi, J. C. Yao, S. Worah, K. Xie, P. F. Mansfield, J. A. Ajani, A. Rashid, S. R. Hamilton, T. T. Wu, Prognostic significance of CpG island methylator phenotype and microsatellite instability in gastric carcinoma. *Clin. Cancer Res.* **11**, 656–663 (2005).
31. N. Oue, Y. Oshimo, H. Nakayama, R. Ito, K. Yoshida, K. Matsusaki, W. Yasui, DNA methylation of multiple genes in gastric carcinoma: Association with histological type and CpG island methylator phenotype. *Cancer Sci.* **94**, 901–905 (2003).
32. E. Yamamoto, H. Suzuki, H. Takamaru, H. Yamamoto, M. Toyota, Y. Shinomura, Role of DNA methylation in the development of diffuse-type gastric cancer. *Digestion* **83**, 241–249 (2011).
33. J. C. Newman, A. M. Weiner, L2L: A simple tool for discovering the hidden significance in microarray expression data. *Genome Biol.* **6**, R81 (2005).
34. I. Ben-Porath, M. W. Thomson, V. J. Carey, R. Ge, G. W. Bell, A. Regev, R. A. Weinberg, An embryonic stem cell–like gene expression signature in poorly differentiated aggressive human tumors. *Nat. Genet.* **40**, 499–507 (2008).
35. E. Kaminskas, A. T. Farrell, Y. C. Wang, R. Sridhara, R. Pazdur, FDA drug approval summary: Azacitidine (5-azacytidine, Vidaza) for injectable suspension. *Oncologist* **10**, 176–182 (2005).
36. K. Yamashita, S. Upadhyay, M. Osada, M. O. Hoque, Y. Xiao, M. Mori, F. Sato, S. J. Meltzer, D. Sidransky, Pharmacologic unmasking of epigenetically silenced tumor suppressor genes in esophageal squamous cell carcinoma. *Cancer Cell* **2**, 485–495 (2002).
37. M. Shiraishi, A. Sekiguchi, A. J. Oates, M. J. Terry, Y. Miyamoto, *HOX* gene clusters are hotspots of de novo methylation in CpG islands of human lung adenocarcinomas. *Oncogene* **21**, 3659–3662 (2002).
38. N. Deng, L. K. Goh, H. Wang, K. Das, J. Tao, I. B. Tan, S. Zhang, M. Lee, J. Wu, K. H. Lim, Z. Lei, G. Goh, Q. Y. Lim, A. L. Tan, D. Y. Sin Poh, S. Riahi, S. Bell, M. M. Shi, R. Linnartz, F. Zhu, K. G. Yeoh, H. C. Toh, W. P. Yong, H. C. Cheong, S. Y. Rha, A. Boussioutas, H. Grabsch, S. Rozen, P. Tan, A comprehensive survey of genomic alterations in gastric cancer reveals systematic patterns of molecular exclusivity and co-occurrence among distinct therapeutic targets. *Gut* **61**, 673–684 (2012).
39. B. P. Berman, D. J. Weisenberger, J. F. Aman, T. Hinoue, Z. Ramjan, Y. Liu, H. Noushmehr, C. P. Lange, C. M. van Dijk, R. A. Tollenaar, D. Van Den Berg, P. W. Laird, Regions of focal DNA hypermethylation and long-range hypomethylation in colorectal cancer coincide with nuclear lamina-associated domains. *Nat. Genet.* **44**, 40–46 (2011).
40. X. Zhang, M. Wu, H. Xiao, M. T. Lee, L. Levin, Y. K. Leung, S. M. Ho, Methylation of a single intronic CpG mediates expression silencing of the *PMP24* gene in prostate cancer. *Prostate* **70**, 765–776 (2010).
41. B. Li, M. Carey, J. L. Workman, The role of chromatin during transcription. *Cell* **128**, 707–719 (2007).
42. M. P. Ball, J. B. Li, Y. Gao, J. H. Lee, E. M. LeProust, I. H. Park, B. Xie, G. Q. Daley, G. M. Church, Targeted and genome-scale strategies reveal gene-body methylation signatures in human cells. *Nat. Biotechnol.* **27**, 361–368 (2009).
43. T. A. Rauch, X. Wu, X. Zhong, A. D. Riggs, G. P. Pfeifer, A human B cell methylome at 100–base pair resolution. *Proc. Natl. Acad. Sci. U.S.A.* **106**, 671–678 (2009).
44. S. Enomoto, T. Maekita, T. Tsukamoto, T. Nakajima, K. Nakazawa, M. Tatematsu, M. Ichinose, T. Ushijima, Lack of association between CpG island methylator phenotype in human gastric cancers and methylation in their background non-cancerous gastric mucosae. *Cancer Sci*. **98**, 1853–1861 (2007).
45. H. Y. Chen, B. H. Zhu, C. H. Zhang, D. J. Yang, J. J. Peng, J. H. Chen, F. K. Liu, Y. L. He, High CpG island methylator phenotype is associated with lymph node metastasis and prognosis in gastric cancer. *Cancer Sci.* **103**, 73–79 (2012).
46. Y. Schlesinger, R. Straussman, I. Keshet, S. Farkash, M. Hecht, J. Zimmerman, E. Eden, Z. Yakhini, E. Ben-Shushan, B. E. Reubinoff, Y. Bergman, I. Simon, H. Cedar, Polycomb-mediated methylation on Lys27 of histone H3 pre-marks genes for de novo methylation in cancer. *Nat. Genet.* **39**, 232–236 (2007).
47. B. H. Min, J. M. Bae, E. J. Lee, H. S. Yu, Y. H. Kim, D. K. Chang, H. C. Kim, C. K. Park, S. H. Lee, K. M. Kim, G. H. Kang, The CpG island methylator phenotype may confer a survival benefit in patients with stage II or III colorectal carcinomas receiving fluoropyrimidine-based adjuvant chemotherapy. *BMC Cancer* **11**, 344 (2011).
48. M. Tasaki, K. Shimada, H. Kimura, K. Tsujikawa, N. Konishi, ALKBH3, a human AlkB homologue, contributes to cell survival in human non-small-cell lung cancer. *Br. J. Cancer* **104**, 700–706 (2011).
49. B. I. Ferreira, J. F. García, J. Suela, M. Mollejo, F. I. Camacho, A. Carro, S. Montes, M. A. Piris, J. C. Cigudosa, Comparative genome profiling across subtypes of low-grade B-cell lymphoma identifies type-specific and common aberrations that target genes with a role in B-cell neoplasia. *Haematologica* **93**, 670–679 (2008).
50. S. Kalari, G. P. Pfeifer, Identification of driver and passenger DNA methylation in cancer by epigenomic analysis. *Adv. Genet.* **70**, 277–308 (2010).
51. T. Ushijima, Epigenetic field for cancerization. *J. Biochem. Mol. Biol.* **40**, 142–150 (2007).
52. A. B. Olshen, E. S. Venkatraman, R. Lucito, M. Wigler, Circular binary segmentation for the analysis of array-based DNA copy number data. *Biostatistics* **5**, 557–572 (2004).
53. Y. Benjamini, Y. Hochberg, Controlling the false discovery rate: A practical and powerful approach to multiple testing. *J. R. Statist. Soc. B* **57**, 289–300 (1995).
54. Q. L. Li, K. Ito, C. Sakakura, H. Fukamachi, K. Inoue, X. Z. Chi, K. Y. Lee, S. Nomura, C. W. Lee, S. B. Han, H. M. Kim, W. J. Kim, H. Yamamoto, N. Yamashita, T. Yano, T. Ikeda, S. Itohara, J. Inazawa, T. Abe, A. Hagiwara, H. Yamagishi, A. Ooe, A. Kaneda, T. Sugimura, T. Ushijima, S. C. Bae, Y. Ito, Causal relationship between the loss of *RUNX3* expression and gastric cancer. *Cell* **109**, 113–124 (2002).

Acknowledgments: We thank members of the Duke-NUS Genome Biology Facility for genomic profiling services. **Funding:** Supported by National Medical Research Council grant TCR/001/2007, Biomedical Research Council grant 10/1/24/19/655, and core grants from Duke-National University of Singapore and Cancer Sciences Institute of Singapore to P.T. **Author contributions:** H.Z., N.D., and P.T. wrote the paper. H.Z., N.D., T.I., Y.Z., Y.H.W., Y.W., I.B.T., and Q.L. analyzed the data. T.I., Y.Z., B.W., D.H., N.L., V.G., J.W., and M.L. performed the experiments. W.P.Y., L.K.G., B.T.T., S.R., and P.T. supervised the research. **Competing interests:** The authors declare that they have no competing interests. **Data and materials availability:** The methylation array data have been deposited in the National Center for Biotechnology Information GEO database under accession number GSE30601.

Submitted 19 June 2012
Accepted 20 August 2012
Published 17 October 2012
10.1126/scitranslmed.3004504

Citation: H. Zouridis, N. Deng, T. Ivanova, Y. Zhu, B. Wong, D. Huang, Y. H. Wu, Y. Wu, I. B. Tan, N. Liem, V. Gopalakrishnan, Q. Luo, J. Wu, M. Lee, W. P. Yong, L. K. Goh, B. T. Teh, S. Rozen, P. Tan, Methylation subtypes and large-scale epigenetic alterations in gastric cancer. *Sci. Transl. Med.* **4**, 156ra140 (2012).